The Journal of Experimental Biology 213, 613-620

doi:10.1242/jeb.037085

Distinct startle responses are associated with neuroanatomical differences in pufferfishes

A. K. Greenwood[1,2,*], C. L. Peichel[1] and S. J. Zottoli[2,3]

[1]Division of Human Biology, Fred Hutchinson Cancer Research Center, Seattle WA, USA [2]Marine Biological Laboratory, Woods Hole MA, USA and [3]Department of Biology, Williams College, Williamstown MA, USA

*Author for correspondence (akg@stanfordalumni.org)

Accepted 16 November 2009

SUMMARY

Despite the key function of the Mauthner cells (M-cells) in initiating escape responses and thereby promoting survival, there are multiple examples of M-cell loss across the teleost phylogeny. Only a few studies have directly considered the behavioral consequences of naturally occurring M-cell variation across species. We chose to examine this issue in pufferfishes, as previous research suggested that there might be variability in M-cell anatomy in this group of fish. We characterized the M-cell anatomy and fast-start responses of two pufferfish species, *Tetraodon nigroviridis* and *Diodon holocanthus*. *T. nigroviridis* showed robust fast-starts to both tactile and acoustic startling stimuli. These fast-starts occurred with a latency typical of M-cell initiation in other fish, and retrograde labeling of spinal-projection neurons revealed that *T. nigroviridis* does have M-cells. By contrast, *D. holocanthus* only rarely exhibited fast-start-like behavior, and these responses were at a substantially longer latency and were much less extensive than those of *T. nigroviridis*. Using three complementary anatomical techniques we were unable to identify obvious M-cell candidates in *D. holocanthus*. These results provide a clear correlation between M-cell presence or absence and dramatic differences in fast-start behavior. The rich diversity within the pufferfish clade should allow future studies investigating the factors that contribute to this correlated anatomical and behavioral variation.

Key words: evolution, fish, behavior, neuroanatomy, escape.

INTRODUCTION

The spectacular array of behaviors exhibited by animals has been generated through the processes of evolution. Behavioral modifications are ultimately produced by differences in neural circuits, but what specific circuitry changes contribute to behavioral evolution? What are the mechanisms by which evolution shapes the structure of these circuits? What constraints dictate how circuits can respond to specific selective pressures? Probing the causes and consequences of nervous system evolution requires a tractable neural circuit and a group of animals that exhibit variation in this circuit (for review, see Carr et al., 2001; Katz and Harris-Warrick, 1999; Nishikawa, 1997; Rose, 2004; Tierney, 1996; Wright, 2000). The circuitry that generates escape behavior in teleost fishes presents such a system.

The escape response, also known as the fast-start or startle response, is initiated by a pair of large, identifiable neurons in the hindbrain: the Mauthner or M-cells (reviewed by Eaton et al., 2001; Korn and Faber, 2005; Zottoli and Faber, 2000). Fast-starts in most teleost fish consist of a C-type fast-start (C-start), the first stage of which is characterized by a rapid unilateral contraction of trunk musculature leading to head and tail movement, which causes the fish to bend into a C-shape. Stage 1 is typically followed by subsequent movements, including a tail stroke that results in a forward propulsion of the center of mass (stage 2), and either gliding or a burst swim (stage 3) (Domenici and Blake, 1997; Eaton et al., 1981; Foreman and Eaton, 1993). M-cell activity precedes the C-start, and electrical stimulation of Mauthner axons can elicit a C-start (Nissanov et al., 1990; Zottoli, 1977). However, M-cells are not necessary for the production of a C-start. When M-cells in goldfish or zebrafish are ablated, a C-start can be elicited, although the onset of the response is delayed (DiDomenico et al., 1988; Eaton et al., 1982; Liu and Fetcho, 1999; Zottoli et al., 1999).

Although considered a key example of a highly conserved ‘identifiable neuron’, M-cells exhibit substantial diversity within teleosts (Bierman et al., 2009; Stefanelli, 1980; Zottoli, 1978a). M-cells can be identified in the majority of teleosts, but many species across the teleost phylogeny lack obvious M-cells or possess M-cells with altered anatomy (Stefanelli, 1980; Zottoli, 1978a). Variable M-cell morphologies include a substantially smaller size, smaller axon diameter or differences in the structure of the axon cap, which is a collection of inhibitory and excitatory fibers that surround the initial segment and axon hillock regions of the M-cell (Bierman et al., 2009; Stefanelli, 1980; Zottoli, 1978a). In some cases, the discovery of small or missing M-cells has been associated with specific types of life history variation, including bottom dwelling and the use of crypsis or camouflage as an anti-predator strategy (e.g. toadfish, flounder, lumpfish), or the extreme modification of caudal fin anatomy (e.g. seahorse, pipefish, ocean sunfish) (Marshall, 1971; Stefanelli, 1980; Uchihashi et al., 1960; Zottoli, 1978a).

Given the diverse anatomy of M-cells among fishes, an outstanding question is how does this natural variation affect fast-start behavior? Only a single published study has directly examined the fast-start behavior of fish with missing M-cells (Hale, 2000). Lumpfish larvae exhibit significantly delayed C-starts when compared to larval zebrafish (Hale, 2000), which is consistent with predictions from M-cell ablation studies (Eaton et al., 1982; Zottoli et al., 1999). However, this study compared fish species across vast phylogenetic scales, and there may be a host of other factors that contribute to the observed behavioral differences.

Pufferfishes, which comprise two sister families within the Order Tetraodontiformes, offer a useful system for further exploring the behavioral consequences of M-cell loss. Pufferfishes exhibit a suite of adaptations in anti-predator defenses, including the capacity to harbor the neurotoxin tetrodotoxin and inflation behavior. These anti-predator innovations might be predicted to alter selection on an ancestral anti-predator behavior, the fast-start. In support of this hypothesis, the only two species of pufferfish that have been previously examined do not perform a fast-start response to a tactile stimulus (Brainerd and Patek, 1998). In addition, anatomical evidence suggests that some pufferfish lack M-cells (Otsuka, 1964; Zottoli, 1978b). However, in several other pufferfish species, M-cells are evident but apparently reduced in size relative to other teleosts (Stefanelli, 1980; Uchihashi et al., 1960).

Several questions arise from this prior work, which could provide insight into M-cell and fast-start evolution. From these previous studies it was unclear whether the lack of M-cells was associated with the absence of fast-start behavior within a single species. In addition, no pufferfish were previously shown to exhibit fast-starts; therefore the function of the M-cells identified in some species was uncertain. Here, we examined fast-start responses using high-speed video and M-cell anatomy using both retrograde labeling and serial plastic sections in two species from the two pufferfish families: *Tetraodon nigroviridis* Marion de Procé (green spotted puffer, Family Tetraodontidae) and *Diodon holocanthus* Linnaeus (porcupine puffer or balloonfish, Family Diodontidae).

MATERIALS AND METHODS

Animals

Choice of species

Tetraodon nigroviridis is closely related to, and often confused with, *T. fluviatilis*, which was previously found to have identifiable, but small, M-cells (Stefanelli, 1980; Tagliani, 1905). *Diodon holocanthus* does not exhibit a fast-start in response to tactile stimulation (Brainerd and Patek, 1998), but its M-cell anatomy has not been previously described.

Housing conditions

Fish were obtained through the aquarium trade (*T. nigroviridis*: Aquariumfish.net; *D. holocanthus*: Sea Dwelling Creatures and Saltwaterfish.com) and were housed at both the Marine Biological Laboratory (MBL) and the Fred Hutchinson Cancer Research Center (FHCRC). *Tetraodon nigroviridis* were housed in brackish water at 15 p.p.t. and *D. holocanthus* were housed in either filtered seawater (MBL) or artificial sea water (FHCRC; Instant Ocean, Aquarium Systems, Mentor, OH, USA). Fish were fed freeze-dried or frozen krill every other day (Hikari, Hayward, CA, USA). All animals were treated in accordance with the Institutional Animal Care and Use Committees at the MBL (protocol #07-07E) and FHCRC (protocol #1781).

Behavior

The startle responses of six *T. nigroviridis* and six *D. holocanthus* individuals were recorded using high-speed videography at 500 frames per second. Two different high-speed cameras were used over the course of the experiment: Fastcam-PCI (Photron, San Diego, CA, USA) and 1200hs (The Cooke Corporation, Romulus, MI, USA). An acrylic aquarium (22 cm×14 cm×13 cm) was positioned on top of a platform, and a mirror that was placed above the tank at a 45 deg. angle enabled the top view to be recorded with the camera positioned horizontally. Fish were presented with four or five trials of tactile and acoustic stimuli, which were randomly interleaved and presented at a minimum of 3-min intervals. The tactile stimulus consisted of a sudden touch to the body using an opaque plastic rod (20 cm×1 cm). The responses to tactile stimuli were not analyzed quantitatively because it was difficult to determine when the tactile stimulus actually made contact with the fish; however, in both species the behavior evoked by this stimulus was qualitatively similar to that evoked by the acoustic stimulus (see Results).

Each fish received two acoustic trials, with the exception of one *D. holocanthus* individual that had three trials. The acoustic stimulus was provided by the impact of a rubber mallet (340 g) on the side of the platform holding the tank. The mallet was suspended next to the platform and was raised to the same height for each trial in order to provide a consistent stimulus.

We quantified several parameters of fast-start behavior from acoustic stimulus trials. We measured some components that are known to be M-cell mediated, as defined by the fact that they are consistently affected by experimental M-cell ablation (latency and probability of the response) (Eaton et al., 1982; Liu and Fetcho, 1999; Zottoli et al., 1999). In addition, we measured components that probably involve the contribution of additional hindbrain neurons (stage 1 duration and angle and peak angular velocity) (Foreman and Eaton, 1993). The probability of a fast-start was determined for each species by dividing the total number of trials evoking a fast-start by the total number of trials (*T. nigroviridis*, 12 trials: six fish with two trials each; *D. holocanthus*, 13 trials: five fish with two trials each and one fish with three trials). For additional quantification of behavior, imported video files were compiled into image stacks in ImageJ Software (NIH, Bethesda, MD, USA). Latency was determined by counting the number of 2 ms frames from the visible impact of the mallet with the apparatus to when the fish commenced axial movement of the head or tail. The end of stage 1 was delineated by the fish beginning to straighten its tail and, in some cases, to turn its head in the opposite direction (Domenici and Blake, 1997; Hale et al., 2002). Although the transition from stage 1 was not as rapid for *D. holocanthus* (see Results), it was nevertheless an obvious change in movement. To quantify the amount and direction of movement during the C-start, we measured the turning angle of each fish during the response (Foreman and Eaton, 1993; Zottoli et al., 1999). Using ImageJ, a line was extended along the midline of the anterior portion of the fish and the change in angle of this line at the end of stage 1, and 10 ms and 70 ms after movement onset was measured [escape trajectory angle (Foreman and Eaton, 1993)]. These values were also used to calculate the peak angular velocity at 4 ms intervals during stage 1. The minimum straight-line distance between the position of each fish before the onset of movement and after 70 ms was also measured (Zottoli et al., 1999). To do this, an identifiable point on the fish (on the midline directly in between the pectoral fins) was tracked rather than the exact center of mass, which was not determined in this study.

Statistical analysis was performed using R statistical software (http://www.r-project.org). Fisher's exact test was used to compare the proportion of trials in which individuals of each species exhibited a C-start. Owing to the small number of *D. holocanthus* fast-starts that were recorded (see Results: three responses from two animals), we did not perform statistical tests on other behavioral measures.

Neuroanatomy

Retrograde tracing

The spinal cords of eleven *T. nigroviridis* (3.9–5 cm standard length) and eight *D. holocanthus* (5.8–8.1 cm standard length) were cut and back-filled with biotin dextran amine (BDA) to identify all cells

that project from the brain into the spinal cord, including the M-cells. Fish were anesthetized in 0.03% MS-222 and were maintained under anesthesia during the surgery. An incision was made in the skin, and muscle and bone were removed in order to expose the spinal cord. The spinal cord was cut using iridectomy scissors, and a solution of biotin dextran amine (Invitrogen, Carlsbad, CA, USA) that had resolidified onto a thin wire was applied onto the cut surface of the cord. The spinal cord was cut 1–4 mm behind the base of the cerebellum (pufferfishes have extremely short spinal cords). There was no difference in the extent of labeling in preparations that had tracer placement varying within this range (data not shown). Following tracer application, the incision was closed with sutures and Vetbond (3M Animal Care Products, St Paul, MN, USA). After 2–3 days, fish were anesthetized in 0.03% MS-222 and perfused with fixative [4% formaldehyde, 1.25% glutaraldehyde in 0.1 mol l^{-1} phosphate buffer, pH 7.4 (PB)]. Brains were removed, post-fixed for 4 h, equilibrated in 30% sucrose in PB, embedded in OCT (Sakura Finetek, Torrance, CA, USA), frozen, and sectioned at 50 μm using a cryostat. Brains were sectioned in horizontal, sagittal or transverse planes. Free-floating sections were then processed to detect BDA using a Vector ABC kit (Vector Laboratories, Burlingame, CA, USA) and DAB as a chromagen with nickel intensification. Sections were processed as follows: 10 min in 3% hydrogen peroxide/10% methanol in PB, 5 min in PB, 2× 5 min in PB with 0.2% Triton X-100 (PBT), 3 h in ABC reagent in PBT, 2× 5 min in PBT, 5 min in PB, 3× 5 min in 0.05 mol l^{-1} Tris, pH 8.4, 15 min in DAB presoak (0.4% DAB, 0.4% nickel ammonium sulfate in Tris), DAB reaction (DAB presoak with 0.015% H_2O_2), then 3× 5 min in cold 0.05 mol l^{-1} Tris, pH 8.4. Sections were then transferred to 0.1 mol l^{-1} PB, mounted on gelatin-subbed slides, counterstained with Cresyl Violet, dehydrated and a coverslip was placed on top. All chemicals were from Sigma (St Louis, MO, USA) unless otherwise indicated.

Silver stain and plastic sections

Two *T. nigroviridis* (3.9 and 4.1 cm standard length) brains and one *D. holocanthus* (8.1 cm standard length) brain were prepared for silver staining. Fish were anesthetized in 0.03% MS-222. Brains were removed and immersed in AFA fixative (9 parts 80% ethanol, 5 parts formalin, 5 parts glacial acetic acid), then dehydrated, cleared in methyl salicylate, embedded in paraffin, sectioned at 15 μm, and stained with Morse's modification of Bodian's silver technique.

One *T. nigroviridis* (3.2 cm standard length) and one *D. holocanthus* (8 cm standard length) brain were embedded in plastic for thin sectioning. Fish were initially anesthetized in 0.03% MS-222 and were then maintained in 0.012% MS-222 during perfusion with 2.5% glutaraldehyde and 1% paraformaldehyde in 0.15 mol l^{-1} sodium cacodylate (pH 7.2). The brains were removed and placed in fresh fixative for 1–2 h, washed in buffer, post-fixed in 2% OsO_4 in 0.15 mol l^{-1} sodium cacodylate for 4 h, washed in buffer, dehydrated in ethanol, cleared in propylene oxide and embedded in Epon. Serial transverse sections (1–2 μm) were mounted on slides, stained with Toluidine Blue and observed with a conventional light microscope.

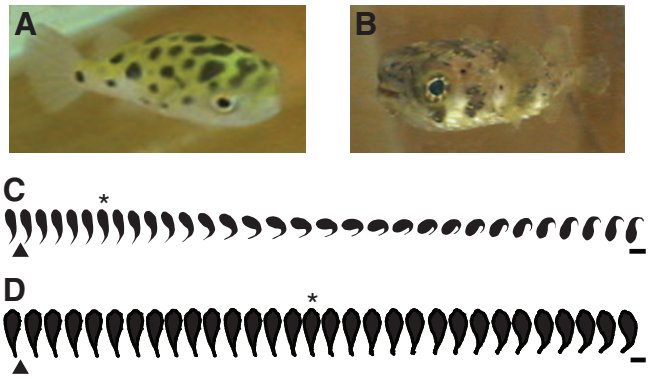

Fig. 1. Comparison of fast-start behavior in *T. nigroviridis* and *D. holocanthus*. Photographs of (A) *T. nigroviridis* (size range: 3.9–5 cm) and (B) *D. holocanthus* (size range: 5.8–8.1 cm). Silhouettes of (C) *T. nigroviridis* and (D) *D. holocanthus* traced from high-speed videos of representative responses to startling acoustic stimulus presentation, as viewed from above. Silhouettes are at 2 ms intervals. The onset of the stimulus is indicated by an arrowhead. The asterisk indicates the latency of the response, determined by the first occurrence of lateral head and/or tail movement. Scale bars, 2 cm.

RESULTS

Behavior

Six *T. nigroviridis* individuals were presented with abrupt tactile and auditory stimuli in order to elicit startle responses. All fish readily produced fast-starts to both types of stimuli. An example of a fish exhibiting a fast-start to the auditory stimulus is shown in Fig. 1. These responses were C-type fast-starts (C-starts), in which the fish assumed a C-shape during the first stage of the response. C-starts had a rapid onset of approximately 11 ms after the auditory stimulus (Table 1). Superficially similar fast-start behavior was elicited following a tactile stimulus, although the latency of this response could not be determined (see Materials and Methods). Thus, *T. nigroviridis* exhibits robust fast-start behavior with a short latency that is suggestive of M-cell initiation (Eaton et al., 1977). Following stage 1, fish exhibited a propulsive tail stroke (stage 2) followed by either gliding or a burst swim (stage 3). The first stage consisted of a variable amount of turning (up to 180 deg.), evidenced by the large variation in the angle traveled during stage 1 (Table 1).

Diodon holocanthus, by contrast, did not show robust fast-start responses. Six fish were tested with both tactile and auditory stimuli.

Table 1. Comparison of fast-start behavior between species

	T. nigroviridis	*D. holocanthus*
C-starts to acoustic stimuli (number of trials)	12/12 (100%)	3/13 (23%)
Latency of movement onset	11.2±1.3 ms	27.3±1.2 ms
Angle 10 ms after onset	42.3±10 deg.	7.8±4 deg.
Duration of stage 1	23.5±9 ms	77±17 ms
Angle at end of stage 1	97.1±55 deg.	39±7 deg.
Angle 70 ms after onset	79.4±71 deg.	34.4±4 deg.
Distance moved after 70 ms	4.05±1.3 cm	0.48±0.16 cm
Peak angular velocity	6.1±2 deg. ms^{-1}	0.8±0.3 deg. ms^{-1}

Values mean ± s.d.

In response to the touch of a rod to the head or tail, *D. holocanthus* individuals did not exhibit a fast-start, but instead used their pectoral fins to swim away from the stimulus or initiated a burst swim (data not shown). In the majority of trials with an auditory stimulus, fish did not make any axial bending movements (Table 1). However, we did record three weak responses from two fish that consisted of slight axial contraction resulting in minimal head and tail movement (Fig. 1, Table 1). Although the C form attained by *D. holocanthus* was much more shallow than that of *T. nigroviridis*, we will refer to *D. holocanthus* responses as C-starts for consistency. The probability of performing a C-start was significantly different between species (Table 1, Fisher's exact test: $P<0.001$). *Diodon holocanthus* C-starts occurred at an average latency of 26 ms, which was over twice as long as *T. nigroviridis*, and the duration of stage 1 was substantially longer than that of *T. nigroviridis* (Table 1). The angle at 10 ms after onset, and the angles at the end of stage 1 and after 70 ms were also considerably smaller in *D. holocanthus* (Table 1). *Diodon holocanthus* individuals also achieved a substantially lower peak angular velocity during their responses (Table 1).

Diodon holocanthus was not observed to make a propulsive tail stroke (stage 2) or a burst swim (stage 3) following stage 1. The distance moved 70 ms after the onset of the fast-start was approximately one body length in *T. nigroviridis*, whereas this distance was almost negligible in *D. holocanthus* (Table 1). Thus, the *D. holocanthus* 'fast-start' consists only of a delayed, weak stage 1 with no successive stages of movement.

Neuroanatomy

Of the multiple elements of escape circuit anatomy that might cause differences in the fast-start response, we focused our efforts on identifying the M-cell. Retrograde labeling of axonal projections, silver-stained preparations and thin plastic sections were used to locate M-cells.

Retrograde tracing of cells projecting into the spinal cord with BDA labeled an array of reticulospinal neurons with a segmental arrangement in both *T. nigroviridis* (Fig. 2) and *D. holocanthus* (data not shown) similar to that described in other fish (Lee and Eaton, 1991; Lee et al., 1993). Vestibulospinal cells, which were more lateral than the reticulospinal cells, were also labeled in both species (data not shown). The extent of BDA labeling was similar in *T. nigroviridis* and *D. holocanthus*. In all brains from both species, we were able to clearly identify at least six reticulospinal segments; the seventh and eighth segment were often difficult to discern because of higher background in caudal hindbrain regions. In addition, we counted the number of labeled cells in four horizontally sectioned brains from both species, and found an average of 171 and 165 labeled cells in *T. nigroviridis* and *D. holocanthus*, respectively.

We were able to identify obvious M-cells in all *T. nigroviridis* brains (N=11; Fig. 2). These cells showed hallmarks of M-cells (Lee and Eaton, 1991; Zottoli, 1978b). They were located at the caudal extent of the fifth motor nucleus at the level of the eighth nerve (Fig. 2). They were found in the fourth segment of reticulospinal cells, which probably corresponds to the fourth hindbrain segment

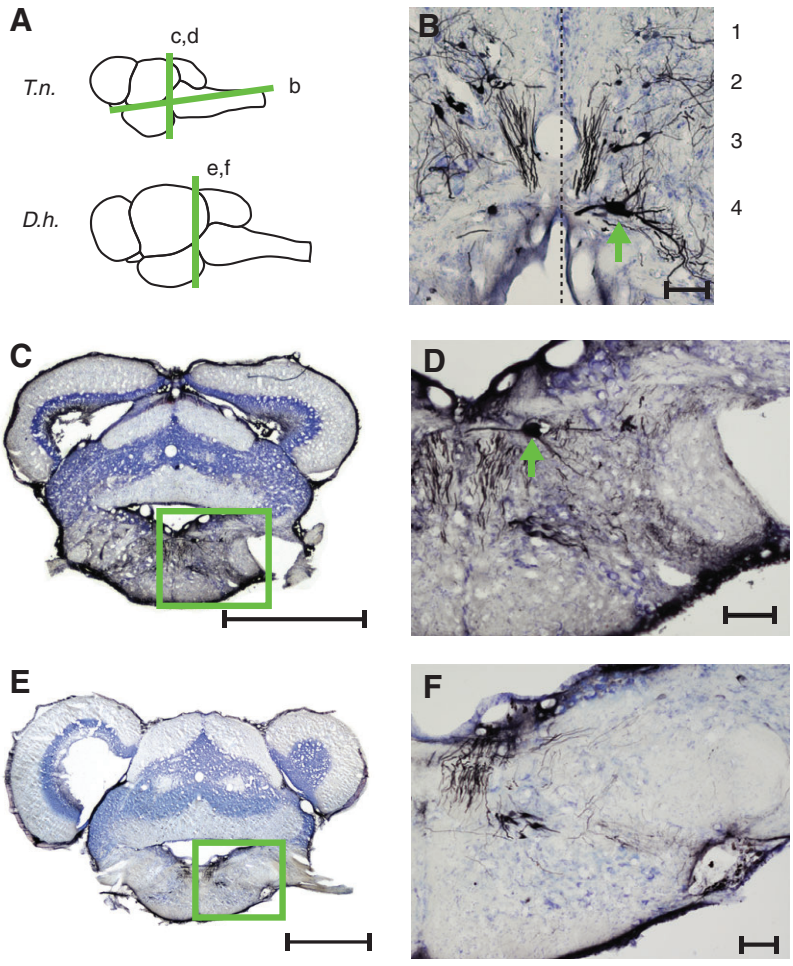

Fig. 2. Comparison of M-cell anatomy in *T. nigroviridis* and *D. holocanthus*. (A) Schematic of brains from each species indicating angle of sections in subsequent panels. *T.n., T. nigroviridis; D.h., D. holocanthus*. (B) Horizontal section from BDA-labeled *T. nigroviridis* brain. The dashed line delineates the midline. DAB-reacted BDA appears black and Nissl counterstain is purple. Hindbrain segments (1–4), delineated by reticulospinal cells, are indicated to the right of this image. A green arrow points to the distinctive M-cell on the right side. Only a small portion of cell body of the left M-cell can be seen in this section. (C) Transverse section from *T. nigroviridis* taken at the caudal extent of the fifth motor nucleus approximately at the level of the eighth nerve. (D) Enlarged view of boxed region in C; the M-cell is indicated by a green arrow. (E) Transverse section from *D. holocanthus* taken at approximately the same position as C. (F) Enlarged view of boxed region in E. No M-cell is visible in this or neighboring sections. Scale bars, 1 mm (C,E) and 100 μm (B,D,F) .

of zebrafish and goldfish (Lee and Eaton, 1991; Lee et al., 1993). The M-cells were substantially larger than all other reticulospinal cells and exhibited a characteristic anatomy, including two large principal dendrites and large axons that crossed the midline (Figs 2, 3). M-cells were clearly distinguishable in silver-stained paraffin sections (data not shown) and Toluidine-Blue-stained plastic sections (Fig. 3). The M-axons were readily identified in the spinal cord (Fig. 4) and could be traced after crossing the midline to the Mauthner cell body on the opposite side of the brain in Toluidine-Blue-stained plastic sections (Fig. 3). The axon cap did not have the features attributed to the 'composite' axon cap of the goldfish and appears more similar to a 'simple' axon cap (Bierman et al., 2009).

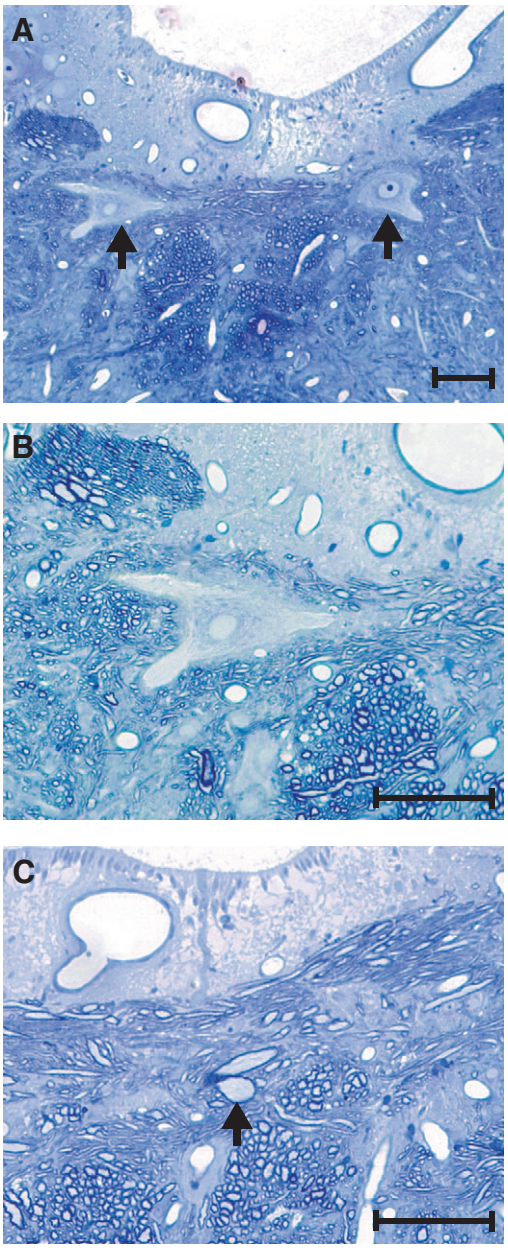

Fig. 3. M-cells and the crossing of the M-axons in *T. nigroviridis*. (A–C) 1 μm cross sections stained with Toluidine Blue. (A) M-cells can be seen on either side of the midline (arrows). Dorsal is up and the midline is in the center of the photograph. (B) Higher power micrograph of the left M-cell. The beginning portion of the lateral dendrite can be seen to the left. The axon hillock and initial segment can be seen to the right. Dorsal is up and the midline is toward the right. (C) The M-axons can be traced caudally where they cross (decussation is designated by an arrow). Dorsal is up and the midline of the spinal cord is in the center of the image. Scale bars, 50 μm.

By contrast, we did not identify any obvious M-cell candidates in *D. holocanthus*. In eight brains, we were unable to distinguish any large retrogradely labeled neurons in the fourth segment of reticulospinal cells at the caudal portion of the fifth motor nucleus (Fig. 2). Careful examination of sections of the spinal cord of *D. holocanthus* from brains that were BDA labeled and Nissl stained (N=8), silver stained (N=1) or Toluidine-Blue stained (N=1) did not reveal any axons that were distinctly larger than other axons (Fig. 4 and data not shown).

The classification of a putative M-cell based solely on anatomical location or size would potentially miss a cell that was substantially modified compared to other fish. Therefore, we expanded our search to account for this possibility. If M-cells were reduced in size but still present in a homologous position, we would nevertheless expect to be able to identify them anatomically because M-cells are characteristically more dorsal than other cells in the fourth reticulospinal segment (see Fig. 2). However, we did not see any smaller, retrogradely labeled cells in this anatomical location that fitted this description. We also evaluated whether large M-cells might indeed be present in the homologous location but that they do not project far enough down the spinal cord to be labeled by a spinal backfill. However, no large cell bodies were distinguishable in this region in *D. holocanthus* in Nissl-stained sections, silver-stained paraffin sections, or Toluidine-Blue-stained thin plastic sections (data not shown).

DISCUSSION

Mauthner cells have a long history of study in comparative neurobiology (Bierman et al., 2009; Stefanelli, 1980; Zottoli, 1978b), although little work has been devoted to studying the behavioral consequences of naturally occurring M-cell loss (Hale, 2000). Our results provide the first correlation between the presence or absence of M-cells and variable fast-start behavior in related species. These findings support and expand classic studies of M-cell ablations in the laboratory (Eaton et al., 1982; Liu and Fetcho, 1999) by examining the behavioral consequences of M-cell loss in an evolutionary context. To our knowledge, this work represents the only published demonstration that naturally occurring M-cell loss in adults is correlated with dramatically altered fast-start behavior.

Using both retrograde labeling of axonal projections and conventional anatomical techniques, we identified distinctive M-cells in *T. nigroviridis* but were unable to distinguish M-cells in *D. holocanthus*. We cannot entirely exclude the possibility that *D. holocanthus* may have atypical M-cells that were missed by our analysis, although we were careful to consider liberal definitions of M-cells in our search. The M-cell was thought to be absent in adult *Xenopus laevis* (Stefanelli, 1951) and freshwater eels (Zottoli, 1978b), but subsequently the M-cell was identified in both (Meredith and Roberts, 1987; Will, 1991). Future work, including developmental analysis or the use of molecular markers (Flores et al., 2008), will be required to definitively confirm that these fish lack M-cells. Our current results suggest that *D. holocanthus* either lacks M-cells or possesses highly atypical M-cells. Therefore, we can confidently conclude that we have identified the presence of M-cells in *T. nigroviridis* and the absence of conserved M-cells in *D. holocanthus*.

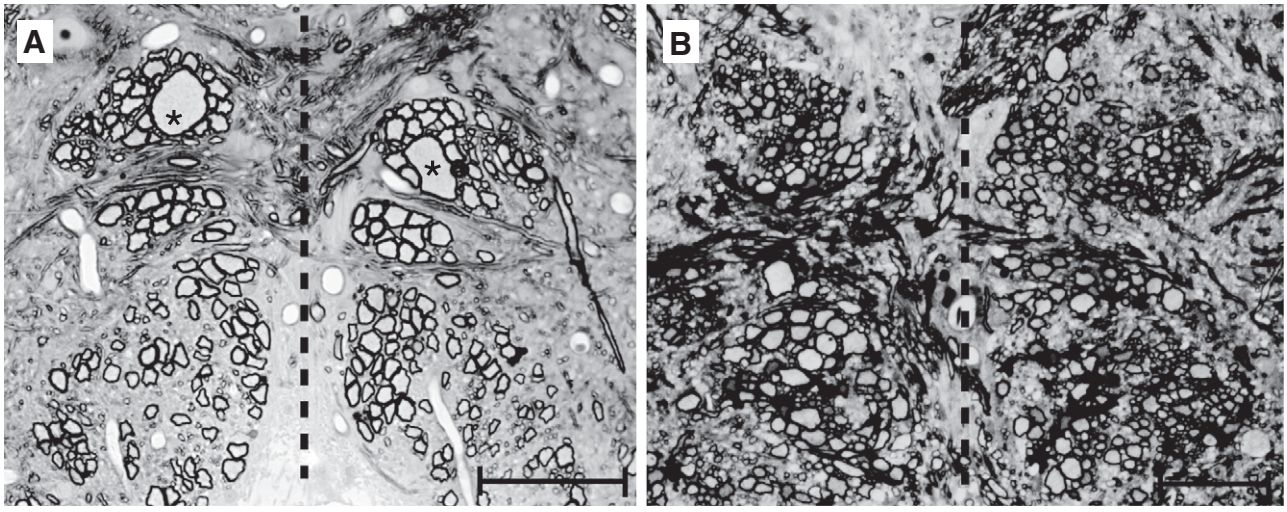

Fig. 4. Comparison of spinally projecting axons in *T. nigroviridis* and *D. holocanthus* at the level of the obex. (A,B) 1 μm cross sections of the fasciculus longitudinalis medialis at the level of the obex, stained with Toluidine Blue, and shown in grayscale. (A) *T. nigroviridis* spinal cord in which the M-axons are easily identified (asterisks). (B) *D. holocanthus* spinal cord in which the M-axons could not be identified. Note that no pair of axons stands out on the basis of size or amount of myelination. Dorsal is up and the midline of the spinal cord is in the center of both images. The position of the midline is indicated with a dashed line. Scale bar, 50 μm.

Differences in M-cell neuroanatomy are correlated with distinctive fast-start behavior in these species. *Tetraodon nigroviridis* performed robust C-type fast-start responses that were similar to M-cell mediated C-starts from other teleosts, including goldfish (Foreman and Eaton, 1993). However, under identical stimulus conditions, *D. holocanthus* only rarely exhibited weak responses at a substantially longer latency. *Diodon holocanthus* may have different stimulus requirements than *T. nigroviridis* or the 'behavioral context' of the animal before the stimulus is delivered might have an influence on the responsiveness of this species (Zottoli et al., 1995). However, in pilot experiments, these fish did not exhibit any rapid trunk movement following presentation of a variety of acoustic, tactile and visual stimuli other than the weak C-start following an acoustic stimulus. *Diodon holocanthus* also did not exhibit fast-starts to a tactile stimulus in a previous study (Brainerd and Patek, 1998).

Several aspects of the behavior of *D. holocanthus* are reminiscent of the fast-start responses of other species of fish with missing M-cells. Compared with *T. nigroviridis*, *D. holocanthus* exhibited a longer latency of movement onset and a reduced probability of performing a C-start. Experimental M-cell ablations result in fast-start responses that occur at a longer latency (Eaton et al., 1982; Kohashi and Oda, 2008; Liu and Fetcho, 1999; Zottoli et al., 1999), and yield a reduced probability of generating a fast-start (Zottoli et al., 1999). In addition, the delayed latency of onset is similar to another species that naturally lacks M-cells (larval lumpfish: Hale, 2000). Although consistent with missing M-cells, a delayed latency alone is not sufficient evidence to indicate the lack of an M-cell. The sea robin has small M-cells and small M-axons (which although small can nevertheless be distinguished, unlike *D. holocanthus*) and exhibits delayed, weak C-starts at a reduced probability compared with goldfish (S.J.Z., unpublished) (Zottoli et al., 1992).

Aside from a reduced probability and longer latency, the behavior of *D. holocanthus* is substantially different from fast-start behavior that typically results from experimental M-cell ablations. *Diodon holocanthus* did not bend as deeply during the C-starts and had a protracted stage 1 duration compared with *T. nigroviridis*, and the peak angular velocity of these responses was dramatically reduced. In addition, *D. holocanthus* essentially did not move away from its initial starting position (i.e. no stage 2) and did not exhibit subsequent stages of movement (i.e. no stage 3) following the weak C-start other than slow relaxation of the C-shape. It is unclear that this response would actually be adaptive for predator avoidance and whether it can be considered a true 'fast-start'.

These substantial kinematic differences suggest that additional factors beyond the lack of identifiable M-cells probably contribute to the distinct behaviors of *D. holocanthus* and *T. nigroviridis*. Besides latency differences, larval lumpfish do not show kinematic differences in their fast-start performance (Hale, 2000). Similarly, M-cell ablations alone do not affect angular, velocity, or distance measures in adult goldfish (Eaton et al., 1982; Zottoli et al., 1999). The altered kinematics of *D. holocanthus* fast-starts could result from additional neuroanatomical and/or morphological factors. The reduced angle and protracted stage 1 duration in *D. holocanthus* suggests that there may be reduced ipsilateral muscle activation (Domenici and Blake, 1997; Foreman and Eaton, 1993). In addition, *D. holocanthus* may lack contralateral muscular activity that typically facilitates a propulsive tail stroke (Domenici and Blake, 1997). These differences imply that other aspects of fast-start circuitry might differ between *D. holocanthus* and *T. nigroviridis*. In larval zebrafish, slight kinematic differences in behavior that are apparent after M-cell ablations are enhanced following additional ablations of the M-cell homologues in adjacent segments (Liu and Fetcho, 1999). It will be interesting to determine if pufferfish possess the M-cell homologues that are found in both goldfish and zebrafish (Kimmel, 1982; Kohashi and Oda, 2008; Lee and Eaton, 1991; Lee et al., 1993), and whether these cells also show anatomical differences between pufferfish species. In addition to variation in neural circuitry, kinematic differences between *D. holocanthus* and *T. nigroviridis* fast-starts could result from morphological differences, including musculature, body shape and body stiffness. The relative contribution of neural *versus* morphological factors to altered fast-start responses can be clarified in the future using electromyography.

Our findings raise interesting evolutionary questions concerning both the loss of M-cells in *D. holocanthus* relative to ancestral teleosts and the variation in M-cells and behavior between the two pufferfish species. The absence of M-cells and robust fast-start behavior in *D. holocanthus* relative to other teleosts could result from a relaxation of selection for the maintenance of fast-start behavior in the presence of a multitude of pufferfish-specific anti-predator adaptations. In addition, the morphological changes that are associated with the gain of inflation include loss of hypaxial musculature (Brainerd, 1994), which may preclude a robust fast-start, leading to a loss of M-cells. The outcome of relaxed selection could vary among species, which might explain the differences in M-cell presence between *T. nigroviridis* and *D. holocanthus*.

Alternatively, there may be direct selection for the loss of a fast-start response and a functional M-cell in *D. holocanthus*. There are obvious tradeoffs between performing a fast-start and generating inflation behavior. Both of these behaviors are used to avoid predation, but a fish cannot perform both fast-start and inflation simultaneously because these behaviors require opposing states of trunk muscle activation (contraction in fast-start and relaxation in inflation). At a neural level, there must be a decision to generate one of the two behaviors in response to a perceived threat. If inflation is consistently a better strategy for *D. holocanthus*, the chance of making the wrong choice (the fast-start) might be selected against. However, potential tradeoffs might be alleviated to some extent if these behaviors are utilized in somewhat different stimulus contexts, for example, initial predator detection *versus* capture. Systematic field observations will be required to assess the relative use of these behaviors in different species.

If the loss of M-cells in *D. holocanthus* is due to selection, *T. nigroviridis* must have experienced a distinct selective regime. These species are from two different pufferfish families, thought to have diverged at least 50 million years ago (Alfaro et al., 2007), and they exhibit multiple differences in morphology, coloration, life history and habitat. At this point, data are lacking from a sufficient number of species to determine whether the presence or absence of M-cells represents the ancestral pufferfish state, so we will discuss the findings in regard to known differences between the two species. As described above, morphological differences between these species may impact fast-start performance, and thereby selection. In addition, because fast-start performance is important in predator escape (Eaton and Hackett, 1984; Walker et al., 2005), an obvious difference to consider between these species is predation pressure. Unfortunately, little is known about the life histories of these species. *Diodon holocanthus* is a marine species, inhabiting mostly inshore and reef habitats throughout the tropics. *T. nigroviridis* is a smaller euryhaline species that resides in estuaries and freshwater streams in the Indo-Pacific. Large bony fish and sharks are known predators of *D. holocanthus* (Leis, 2001; Randall, 1967). Predators of *T. nigroviridis* are not well characterized, but could include both birds and fish, given their size and habitat. Divergence in several characteristics supports the idea that these species may experience different predation regimes. Although both species are known to contain tetrodotoxin (Chen and Chou, 1998; Mahmud et al., 2003), *T. nigroviridis* has a potentially aposematic coloration pattern (Fig. 2), whereas *D. holocanthus* exhibits mottled, disruptive coloration, most likely for camouflage. In addition, our anecdotal laboratory observations suggest that these fish employ inflation behavior to different extents. *Tetraodon nigroviridis* was rarely observed to perform inflation behavior, whereas *D. holocanthus* did so frequently during routine handling.

Although at this stage we cannot pinpoint the key factors that contribute to the species differences, our findings provide a clear foothold into variation in M-cells and correlated fast-start behavior characters in the pufferfish phylogeny. In the future, we can take advantage of the diversity within pufferfish to examine the evolutionary history of and ultimately the mechanisms contributing to the gain or loss of fast-start behavior and circuitry.

ACKNOWLEDGEMENTS

We are grateful to Janice Simmons, Scott Lindell and Shaun McCann for advice and assistance with fish husbandry; to Gwyneth Card, Michael Dickinson and Jason Ritt for assistance with high-speed cameras; and to Tina Wong, Nancy Piatczyc and Farah Musani for technical assistance. This work was supported by a Grass Fellowship and a Helen Hay Whitney Postdoctoral Fellowship to A.K.G., a Burroughs Wellcome Career Award in the Biomedical Sciences to C.L.P. and a Williams College Howard Hughes Medical Institute and Essel Foundation grant to S.J.Z.

REFERENCES

Alfaro, M. E., Santini, F. and Brock, C. D. (2007). Do reefs drive diversification in marine teleosts? Evidence from pufferfishes and their allies (Order Tetraodontiformes). *Evolution* **61**, 2104-2126.

Bierman, H. S., Zottoli, S. J. and Hale, M. E. (2009). Evolution of the Mauthner axon cap. *Brain Behav. Evol.* **73**, 174-187.

Brainerd, E. L. (1994). Pufferfish inflation: functional morphology of postcranial structures in *Diodon holocanthus* (Tetraodontiformes). *J. Morphol.* **220**, 243-261.

Brainerd, E. L. and Patek, S. N. (1998). Vertebral column morphology, C-start curvature, and the evolution of mechanical defenses in Tetraodontiform fishes. *Copeia* **4**, 971-984.

Carr, C. E., Soares, D., Parameshwaran, S. and Perney, T. (2001). Evolution and development of time coding circuits. *Curr. Opin. Neurobiol.* **11**, 727-733.

Chen, C.-Y. and Chou, H.-N. (1998). Detection of tetrodotoxin by high performance liquid chromatography in lined-moon shell and puffer fish. *Acta Zool. Taiwanica* **9**, 41-48.

DiDomenico, R., Nissanov, J. and Eaton, R. C. (1988). Lateralization and adaptation of a continuously variable behavior following lesions of a retiuclospinal command neuron. *Brain Res.* **473**, 15-28.

Domenici, P. and Blake, R. (1997). The kinematics and performance of fish fast-start swimming. *J. Exp. Biol.* **200**, 1165-1178.

Eaton, R. C. and Hackett, J. T. (1984). The role of the Mauthner cell in fast-starts involving escape in teleost fishes. In *Neural Mechanisms of Startle Behavior* (ed. R. C. Eaton), pp. 213-266. New York: Plenum Press.

Eaton, R. C., Bombardieri, R. A. and Meyer, D. L. (1977). The Mauthner-initiated startle response in teleost fish. *J. Exp. Biol.* **66**, 65-81.

Eaton, R. C., Lavender, W. A. and Wieland, C. M. (1981). Identification of Mauthner initiated response patterns in goldfish: evidence from simultaneous cinematography and electrophysiology. *J. Comp. Physiol. A* **144**, 521-531.

Eaton, R. C., Lavender, W. A. and Wieland, C. M. (1982). Alternative neural pathways initiate fast-start responses following lesions of the Mauthner neuron in goldfish. *J. Comp. Physiol. A* **145**, 485-496.

Eaton, R. C., Lee, R. K. and Foreman, M. B. (2001). The Mauthner cell and other identified neurons of the brainstem escape network of fish. *Prog. Neurobiol.* **63**, 467-485.

Flores, C. E., Ene, S. and Pereda, A. E. (2008). An immunohistochemical marker for goldfish Mauthner cells. *J. Neurosci. Methods* **175**, 64-69.

Foreman, M. B. and Eaton, R. C. (1993). The direction change concept for reticulospinal control of goldfish escape. *J. Neurosci.* **13**, 4101-4113.

Hale, M. E. (2000). Startle responses of fish without Mauthner neurons: Escape behavior of the lumpfish (*Cyclopterus lumpus*). *Biol. Bull.* **199**, 180-182.

Hale, M. E., Long, J. H., Jr, McHenry, M. J. and Westneat, M. W. (2002). Evolution of behavior and neural control of the fast-start escape response. *Evolution* **56**, 993-1007.

Katz, P. S. and Harris-Warrick, R. M. (1999). The evolution of neuronal circuits underlying species-specific behavior. *Curr. Opin. Neurobiol.* **9**, 628-633.

Kimmel, C. B. (1982). Reticulospinal and vestibulospinal neurons in the young larva of a teleost fish, *Brachydanio rerio*. In *Progress in Brain Research: Anatomy of Descending Pathways to the Spinal Cord*, vol. 57 (ed. H. G. J. M. Kuypers and G. F. Martin), pp. 1-24. New York: Elsevier Biomedical.

Kohashi, T. and Oda, Y. (2008). Initiation of Mauthner- or non-Mauthner-mediated fast escape evoked by different modes of sensory input. *J. Neurosci.* **28**, 10641-10653.

Korn, H. and Faber, D. S. (2005). The Mauthner cell half a century later: a neurobiological model for decision-making? *Neuron* **47**, 13-28.

Lee, R. K. and Eaton, R. C. (1991). Identifiable reticulospinal neurons of the adult zebrafish, *Brachydanio rerio*. *J. Comp. Neurol.* **304**, 34-52.

Lee, R. K., Eaton, R. C. and Zottoli, S. J. (1993). Segmental arrangement of reticulospinal neurons in the goldfish hindbrain. *J. Comp. Neurol.* **329**, 539-556.

Leis, J. M. (2001). Family Diodontidae. In *FAO Species Identification Guide for Fishery Purposes*, vol. Bony Fishes part 4 (ed. K. E. Carpenter and V. H. Niem), pp. 3958-3965.

Liu, K. S. and Fetcho, J. R. (1999). Laser ablations reveal functional relationships of segmental hindbrain neurons in zebrafish. *Neuron* **23**, 325-335.

Mahmud, Y., Arakawa, O., Ichinose, A., Tanu, M., Takatani, T., Tsuruda, K., Kawatsu, K., Hamano, Y. and Noguchi, T. (2003). Intracellular visualization of tetrodotoxin (TTX) in the skin of a puffer *Tetraodon nigroviridis* by immunoenzymatic technique. *Toxicon* **41**, 605-611.
Marshall, N. B. (1971). *Explorations in the Life of Fishes*. Cambridge, MA: Harvard University Press.
Meredith, G. E. and Roberts, B. L. (1987). Distribution and morphological characteristics of efferent neurons innervating end organs in the ear and lateral line of the European eel. *J. Comp. Neurol.* **265**, 494-506.
Nishikawa, K. C. (1997). Emergence of novel functions during brain evolution. *BioScience* **47**, 341-353.
Nissanov, J., Eaton, R. C. and DiDomenico, R. (1990). The motor output of the Mauthner cell, a reticulospinal command neuron. *Brain Res.* **517**, 88-98.
Otsuka, N. (1964). Weitere vergleichend-anatomische untersuchlungen an Mauthnerschen zellen von fischen. *Z. Zelleforsch.* **62**, 61-71.
Randall, J. E. (1967). Food habits of reef fishes of the West Indies. *Stud. Trop. Oceanogr. Miami* **5**, 665-847.
Rose, G. J. (2004). Insights into neural mechanisms and evolution of behaviour from electric fish. *Nat. Rev. Neurosci.* **5**, 943-951.
Stefanelli, A. (1951). The Mauthnerian apparatus in the Ichthyopsida; its nature and function and correlated problems of neurohistogenesis. *Q. Rev. Biol.* **26**, 17-34.
Stefanelli, A. (1980). I neuroni di Mauthner degli ittiopsidi valutazioni comparative morfologiche e funzionali. *Atti Della Accad. Naz. dei Lincei* **16**, 1-43.
Tagliani, G. (1905). Le fibre del Mauthner nel midollo spinale de'Vertebrati inferiori (anamni). *Arch. Zool.* **2**, 385-435.
Tierney, A. J. (1996). Evolutionary implications of neural circuit structure and function. *Behav. Process.* **35**, 173-182.
Uchihashi, K., Shimamura, H. and Honda, A. (1960). A study on the Mauthner cell in teleosts in relation to the swimming behavior. *Ann. Rept. Jap. Sea Reg. Fish Res. Lab.* **6**, 203-216.
Walker, J. A., Ghalambor, C. K., Griset, O. L., McKenney, D. and Reznick, D. N. (2005). Do faster starts increase the probability of evading predators? *Funct. Ecol.* **19**, 808-815.
Will, U. (1991). Amphibian Mauthner cells. *Brain Behav. Evol.* **37**, 317-332.
Wright, W. G. (2000). Neuronal and behavioral plasticity in evolution: experiments in a model lineage. *BioScience* **50**, 883-894.
Zottoli, S. J. (1977). Correlation of the startle reflex and Mauthner auditory responses in unrestrained goldfish. *J. Exp. Biol.* **66**, 243-254.
Zottoli, S. J. (1978a). Comparative morphology of the Mauthner cell in fish and amphibians. In *Neurobiology of the Mauthner Cell* (eds. D. S. Faber and H. Korn). New York: Raven Press.
Zottoli, S. J. (1978b). Comparison of Mauthner cell size in teleosts. *J. Comp. Neurol.* **178**, 741-757.
Zottoli, S. J. and Faber, D. S. (2000). The Mauthner cell: what has it taught us? *The Neuroscientist* **6**, 25-37.
Zottoli, S. J., Davis, G. W. and Northen, S. C. (1992). Comparative studies of the Mauthner cell in teleosts. *Neurology Today* **1992**, 53-63.
Zottoli, S. J., Bentley, A. P., Prendergast, B. J. and Rieff, H. I. (1995). Comparative studies on the Mauthner cell of teleost fish in relation to sensory input. *Brain Behav. Evol.* **1995**, 151-164.
Zottoli, S. J., Newman, B. C., Rieff, H. I. and Winters, D. C. (1999). Decrease in occurrence of fast startle responses after selective Mauthner cell ablation in goldfish (*Carassius auratus*). *J. Comp. Physiol. A* **184**, 207-218.